BJRS

BRAZILIAN JOURNAL
OF
RADIATION SCIENCES
10-02A (2022) 01-13

SBPR
Sociedade Brasileira de Proteção Radiológica

The potential of protective glass from smartphones as an emergency personal dosimeter for members of the general public in radiological accidents

S. Sholom*, S.W.S. McKeever

Department of Physics, Oklahoma State University, Stillwater, Oklahoma 74074, USA
sergey.sholom@okstate.edu

ABSTRACT

The potential of the back protective glass from modern smartphones as a possible material for an emergency triage, OSL dosimeter was evaluated. Strong OSL signals were observed in samples of glass from phones of different models and brands after irradiation. Some important parameters of these signals were analyzed, namely the OSL decay curve shape, the dependence on dose, and the stability (fading) with time after exposure. Analysis of the shape suggested that the main mechanism of the OSL production is optically assisted tunneling. The dose-response characteristics demonstrated linearity in the tested dose range (0-2.7 Gy) provided that fading was accounted for during calibration irradiation. The fading after irradiation was described by a universal, two-component function with a primary component due to tunneling and a secondary, thermal component. Dose reconstruction tests were carried out for in-service phones exposed to known doses and then kept in normal usage (phone calls, texts, web surfing, etc.) as well as for out-of-service phones irradiated to blind (unknown) doses. Dose reconstruction was conducted using a custom-made OSL reader without dismantling any part of the phone. OSL-reconstructed, fading-corrected doses were within 25% (worse case) of the corresponding nominal values. It was concluded that the back protective glass can be used as an OSL emergency triage dosimeter (if protected from ambient light by a phone case).

Keywords: **Non-destructive OSL dosimetry with phones, Phone protective glass, Tunneling mechanism in OSL.**

ISSN: 2319-0612
DOI: https://10.15392/bjrs.v10i2A.2062
Submitted:2021-05-15
Accepted: 2022-05-16

1. INTRODUCTION

There have been several major radiological accidents in the past, of which may be mentioned the Mayak disaster in Russia (September, 1957), the Chornobyl Nuclear Power Plant (NPP) accident in Ukraine (April, 1986), and the Fukushima NPP accident in Japan (March, 2011) (e.g., [1-3]). In all such accidents, hundreds of thousands of people from the general population were either exposed or potentially exposed to unknown radiation doses. It is evident that in today's modern world, radiological/nuclear accidents are, unfortunately, a fact of life and, were any to happen in the future, they may also affect very large numbers of people.

Assessment of personal doses due to exposure during such events is essential due to the necessity of promptly triaging potentially exposed people. Two different approaches are usually exploited for such a purpose [4-5], namely Biological Dosimetry (i.e. direct estimate of the dose to an individual using biological material (mostly blood)), and Physical Dosimetry (when the dose is first assessed to an object carried by an individual, using electron paramagnetic resonance (EPR), optically stimulated luminescence (OSL) or thermoluminescence (TL) techniques, and is then converted to the dose to the individual, see e.g. [6]). In the latter approach, biologically-derived material (such as teeth and nails), or "fortuitous" material carried by an individual (such as personal electronics and credit cards, see e.g. [7-9]) may be used.

In this paper, we describe a study of back protective glass, which may be found on most current smartphones, as a possible emergency OSL dosimeter. This component of a phone can be measured without dismantling the phone, which is a clear advantage when compared with dosimetry using other phone components like resistors, inductors, integrated circuits. Use of the latter components requires that the phone must be dismantled and destroyed [10-12]. The general TL and OSL properties of the phone protective glass were described in [13-14], and two different non-destruction methods of OSL signal readout were proposed in [15-16]. In the current work, we provide further insight into the nature of the physical mechanism responsible for the OSL signal production in these materials and its stability, as well as presenting results of some dose recovery tests.

2. MATERIALS AND METHODS

The back glasses from eight different smartphones were used for general tests. For these experiments, several aliquots, of size approximately 5 × 5 mm2, were cut from the glasses. Information about these smartphones is given in Table 1.

Smartphone protective glass is made of aluminosilicate glass. The composition and structure of such glass are shown in Figure 1.

Five additional smartphones were used in the dose recovery test. Three out-of-service iPhone XR phones were exposed to blind doses while two in-service iPhone 11 models were irradiated to known laboratory doses. Phones were measured at different times (in the range 3-7 days) after irradiation.

All OSL measurements were conducted on the custom-built OSL reader specially designed to accommodate the entire phone. This reader is described in detail in [16].

Table 1. General information about tested phones

Phone #	Phone model
1	iPhone XR
2	iPhone X
3	iPhone XS
4	iPhone 11
5	iPhone8
6	Samsung Note10
7	LG V30
8	Samsung S10

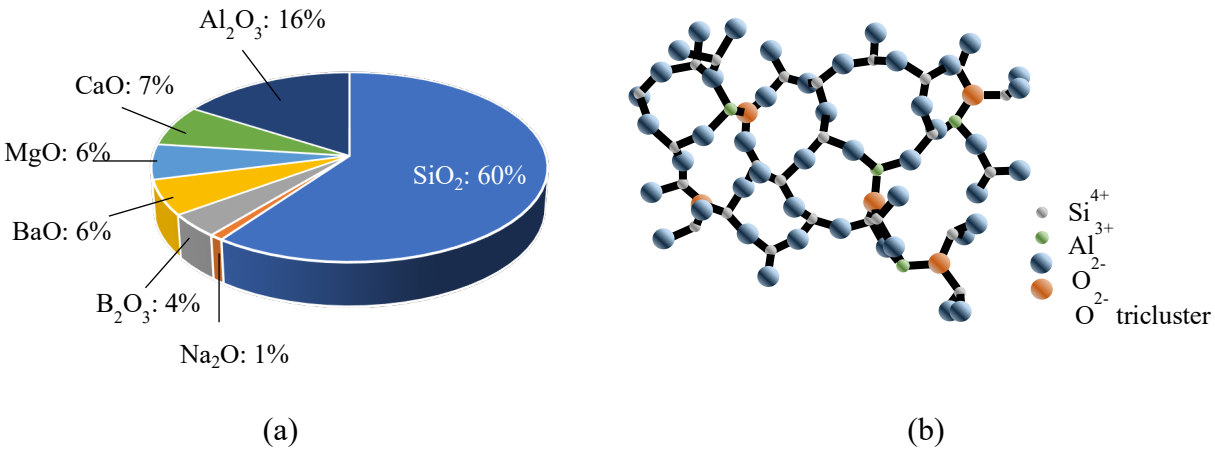

Figure 1: *Composition (a) and structure (b) of aluminosilicate glass usually used for manufacturing of the protective glass.*

CW-OSL decay curves were recorded for stimulation times of 200 s using 200 data points per curve. The dosimetric signal (DS) was calculated as a difference of two OSL integrals: over first- and last 10 s of the curve. Dose-response curves were measured in the dose range 0-2.7 Gy.

Fading of the OSL signal with time after irradiation was studied using irradiation of the phones to a test dose and measurement of the OSL at various times after the exposure. The DSs in this experiment were normalized to the corresponding values observed 3 min after irradiation. The phones after irradiation were stored in the dark assuming that phones kept in opaque cases have similar fading properties.

Different ionizing radiation sources were used for irradiation of samples. For general OSL tests, samples were exposed with an external 90Sr/90Y beta source delivering 20 Gy/min. The in-service phones were irradiated using a Hewlett Packard Faxitron 43805N X-ray system operating at 100 kV and 2.7 mA, and equipped with a 2 mm Al filter. The dose rate at the phone placement was 133 mGy/min. The out-of-service phones were irradiated at BfS (Germany) using a Maxishot SPE X-ray cabin operating at 240 kV and 13 mA, and equipped with a 3 mm beryllium and a 3 mm aluminum filter; the dose rate at the sample position was 1 Gy/min. This irradiation was conducted within the framework of large inter-laboratory comparison performed by RENEB, which involved 46 scientific institutions and 8 different biological and physical dosimetric techniques. (The results

of this inter-comparison are in process of preparation for publication.) After exposure, the phones, in cases, were shipped to the OSL lab and measured immediately after arrival.

All the above doses are referenced to a dose in air.

3. RESULTS AND DISCUSSION

3.1 OSL characteristics

Blue-stimulated OSL curves observed in the tested samples irradiated to a dose of 1 Gy are shown in Fig. 2 for linear (a) and log (b) scales. It is suggested that the experimental OSL curves approximately follow a t-n decay law, which suggests the optically-assisted tunneling (OAT) as a main mechanism of OSL signal production.

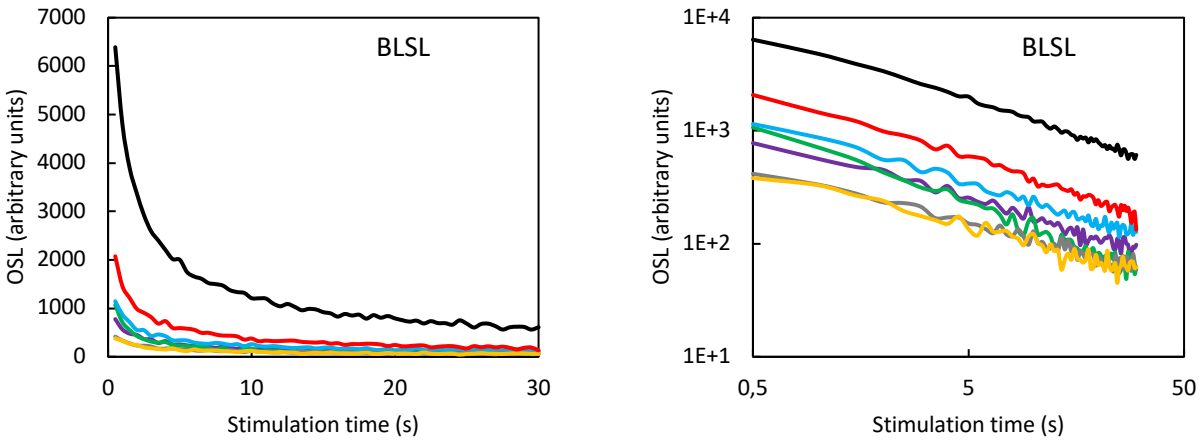

(a) (b)

Figure 2: *Blue-stimulated OSL (BLSL) curves from protective glass from a variety of phones. Irradiation dose 1 Gy; (a) is on a linear scale while (b) is a log scale.*

Tunneling and its effect on TL and OSL have been studied extensively in the past. The main recent papers are [17-19]. The approaches proposed in these papers were applied to analyze the OSL curves obtained for two different stimulation wavelengths, namely, Blue-stimulated and Green-stimulated OSL (BLSL and GLSL, respectively). The results of corresponding fitting are shown in Fig. 3(b)-(d) for normalized intensity in the log scale; Fig. 3(a) shows the original OSLs.

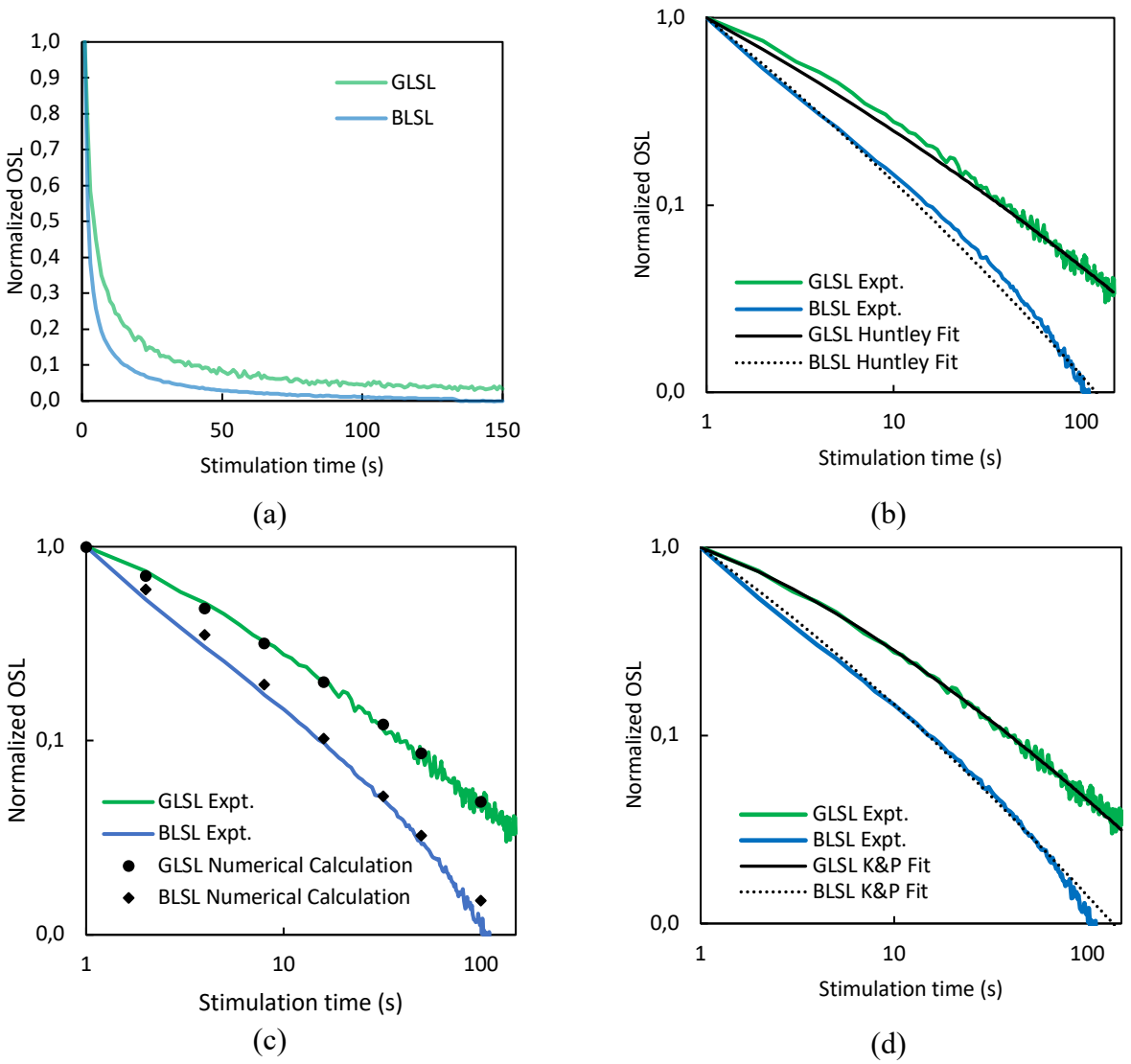

Figure 3: *Fits of the OSL curves obtained for two different stimulation wavelengths (Blue- and Green-stimulated OSL, or BLSL and GLSL) to Huntley model [17] (b), Jain et al. semi-analytical model [18] (c) and Kitis and Pagonis analytical model [19] (d). Plot (a) shows the original OSL curves.*

It is seen in Fig. 3 that there is quite satisfactory fitting for any of the tested models, which suggests that optically-assisted tunneling (OAT) is a dominant mechanism in the OSL signal production, but there is also some discrepancy between experimental and fitting data for any model, which means that, additionally to the OAT, there is another mechanism (secondary mechanism) that also contributes to the OSL. Clarification of this secondary mechanism was beyond the scope of the current work.

Tunneling from the excited state may be represented by a diagram shown in Fig. 4(a); stimulation light excites electron into Band-Tail states, which are distributed in glass, as a disorder material, according to exponential law with density of states described by Urbach's formula [20]:

$$\rho(E) \propto exp\{(E - E_o)/E_U\}$$

where EU is the characteristic width of the band tail states and E_o is the optical trap depth.

Measuring OSL response as a function of stimulation energy (i.e. for different wavelengths of stimulation light), it is possible to determine the parameters E_o and EU. An example of such dependence is shown in Fig. 4(b) for the two tested phones; values of the fitted parameters were E_o = 1.91 eV and 2.02 eV, E_U = 0.30 eV and 0.25 eV for iPhone 11 and iPhone 8, respectively.

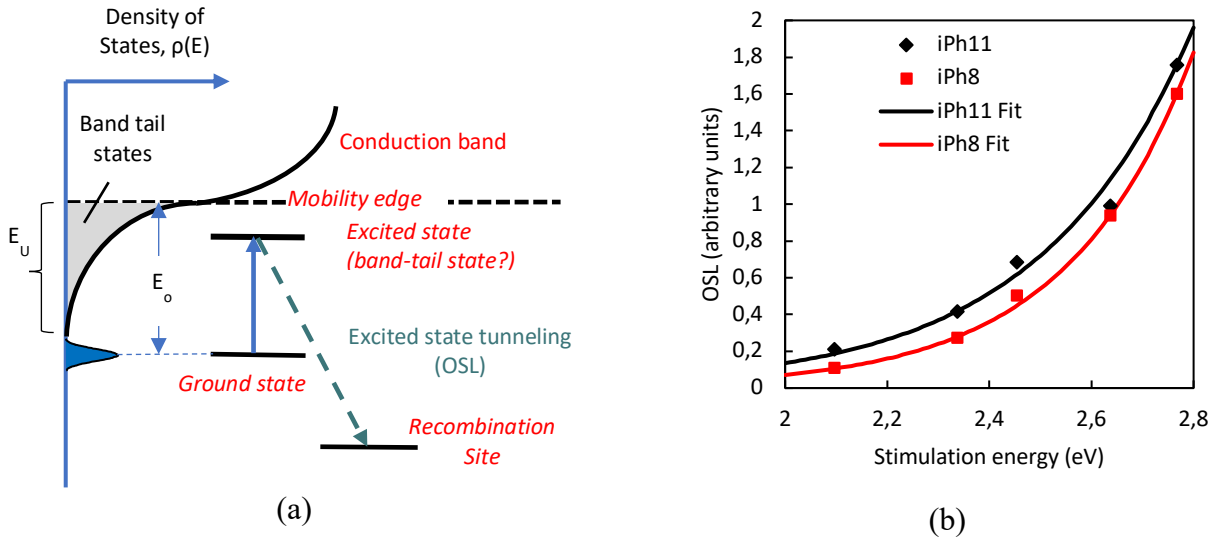

Figure 4: *(a) Model for the excited state tunneling; (b) fit to Urbach's formula for Band-Tail states* $\rho(E) \propto exp\{(E - E_o)/E_U\}$. E_o *= 1.91 eV and 2.02 eV,* E_U *= 0.30 eV and 0.25 eV for iPh11 and iPh8, respectively.*

3.2 Fading considerations

If glass is stored in the dark after irradiation, tunneling may occur directly from the ground state to the recombination level. The corresponding diagram and data are shown in Fig. 5. Fig. 5(a) shows a model for ground-state tunneling, whereas plot (b) demonstrates two OSL curves recorded at different times after irradiation. Additionally, there may be a non-zero thermal component contributing to the fading.

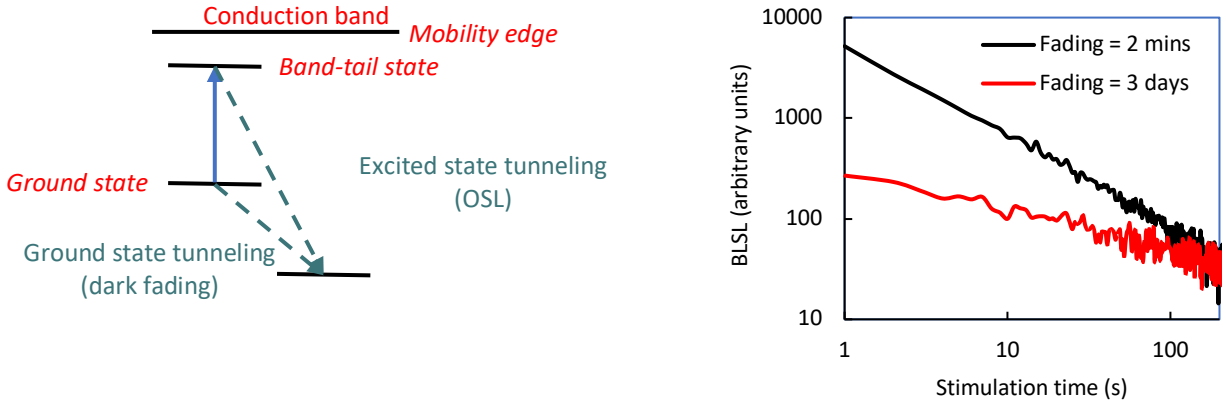

(a) (b)

Figure 5: *(a) Model for the ground state tunneling; (b) examples of OSL curves recorded at different fading times after irradiation.*

To estimate the possible contributions from these two mechanisms the fading curves were obtained for several mobile phones (Fig. 6(a)), and the average fading dependence was fitted by the function:

$$I_{OSL}(t) = A exp\left\{-\frac{t}{\tau}\right\} + Bt^{-n}$$

where the first term describes a thermal component, of temperature-dependent time constant t, while the second term corresponds to the tunneling component. A, B and n are constants. The result of the fitting is shown in Fig. 6(b); it is seen that the tunneling component dominates at the initial phase after exposure, with a small thermal component. Also important observation from Fig. 6 is that the fading of OSL in the glass can be described by a universal curve (a black line in Fig. 6b).

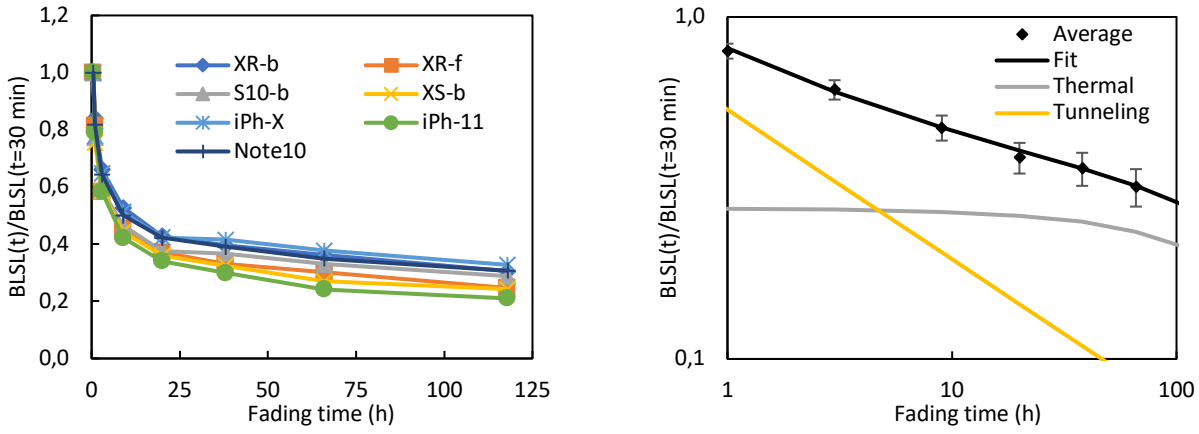

(a) (b)

Figure 6: *(a) Fading of OSL for several mobile phones; (b) fitting of the average fading dependence by a function* $I_{OSL}(t) = Aexp\left\{-\frac{t}{\tau}\right\} + Bt^{-n}$, *where first term describes a thermal component while the second term corresponds to tunneling component.*

1.1. 3.3 Dose-response characteristics

Examples of dose-response characteristics are shown in Fig. 7 for three representative glasses. OSL signals in this test were recorded at the same effective fading time $t_{eff} = t_{irr}/2 + t_{del}$, where irradiation time t_{irr} was varied in the range 1-20 min depending on the chosen dose, and the delay time t_{del} between irradiation and OSL readout was adjusted in such a way that t_{eff} always equalled 30 min.

It is seen in Fig. 7 that the dose-response curves are linear after accounting for fading during calibration irradiation in the above manner. Using the dose-response curves similar to those shown in Fig. 7, the values of the minimum detectable doses were calculated for the tested phones. They were in the range 0.2-5 mGy for the different phones measured 3 min after exposure.

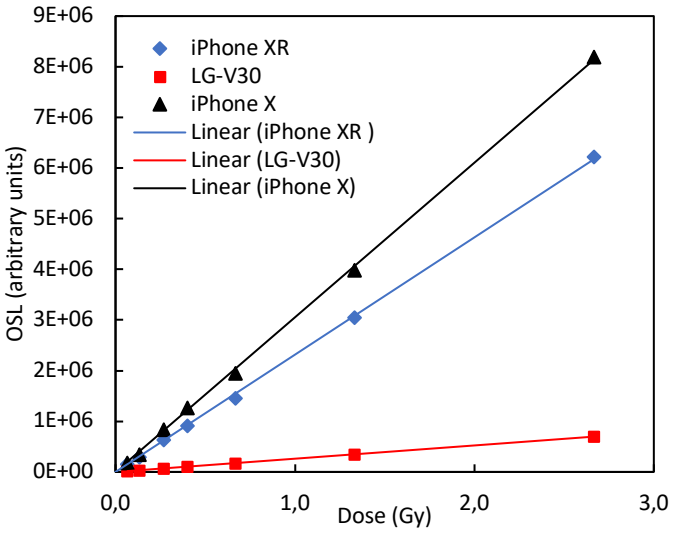

Figure 7: *Dose responses of some representative phone glasses. OSL were recorded at the effective fading time* $t_{eff} = t_{irr}/2 + t_{del}$.

3.4 Dose recovery tests

As was already stated in the Material and Methods Section, several mobile phones were exposed to different known and blind doses using two different X-ray sources and the OSL measured within 3-7 days after irradiation. After measurements, the phones were irradiated to a calibration dose of 0.3 Gy, the OSL was measured again, and the doses were calculated. At the final step, the doses were corrected for fading using the fitted curve from Fig. 6(b). All these steps require just 10-15 min per one phone (two OSL readouts 200 s each, 2 min for calibration irradiation, and few minutes for phone uploading/unloading). The whole procedure doesn't affect the condition of the phone.

The final results of the dose recovery tests are presented in Table 2.

It is seen from the Table 2 that the deviation of the reconstructed, fading-corrected doses from corresponding nominal values is within 25 % (maximum) in the dose range 0.27-3.5 Gy, which is an acceptable value for potential triage applications.

Table 2. Results of the dose recovery tests

Phone #	Nominal dose, Gy	Fading time, days	OSL dose, Gy	Fading coefficient	Corrected dose, Gy	Deviation, %
iPhone 11 #1	0.27 (known)	6	0.028	0.143	0.20	25
iPhone 11 #2	0.27 (known)	7	0.030	0.137	0.22	17
iPhone XR #1	0 (blind)	3.4	0.0	0.189	0	0
iPhone XR #2	1.20 (blind)	3.4	0.21	0.189	1.12	7
iPhone XR #3	3.50 (blind)	3.4	0.53	0.189	2.81	20

CONCLUSIONS

- Back-protective-glass from smartphones can be used as an OSL emergency dosimeter (if protected from ambient light by a phone case).
- The method is simple, non-destructive and rapid (~ 10-15 mins per phone); the phone remains fully functional throughout.
- Fading correction is possible using a universal correction curve.
- Fading-corrected doses shown to be accurate within ~25%, which is quite acceptable for triage.

REFERENCES

[1] DEGTEVA, M.O., ANSPAUGH, L.R., AKLEYEV, A.V., JACOB, P., IVANOV, D.V., WEISER, A., VOROBIOVA, M.I., SHISHKINA, E.A., SHVED, V.A., VOZILOVA, A.V., BAYANKIN, S.N., NAPIER, B. Electron paramagnetic resonance and fluorescence in situ hybridization-based investigations of individual doses for persons living at Metlino in the upper reaches of the Techa River. **Health Phys,** v. 88, p. 139–153, 2005.

[2] CHUMAK, V., SHOLOM, S., PASALSKAYA, L. Application of high precisions EPR dosimetry with teeth for reconstruction of doses to Chernobyl populations. **Radiat Prot Dosim,** v. 84, p. 515-520, 1999.

[3] ISHIKAWA, T. Radiation doses and associated risk from the Fukushima nuclear accident: a review of recent publications. **Asia Pacific J Public Health,** v. 29(2S), p. 18S–28S, 2017.

[4] BAILIFF, I.K., MCKEEVER, S.W.S., SHOLOM, S. Retrospective and emergency dosimetry in response to radiological incidents and nuclear mass-casualty events: a review. **Radiat Meas,** v. 94, p. 83–139, 2016.

[5] ICRU - International Commission on Radiation Units and Measurements. **Methods for Initial-Phase Assessment of Individual Doses Following Acute Exposure to Ionizing Radiation, ICRU Report 94**, J. ICRU, 2019. 162p.

[6] CHANDLER, J.R., SHOLOM, S., MCKEEVER, S.W.S., BAKHANOVA, E., CHUMAK, V., VELÁSQUEZ, D., HALL, H.L. Dose conversion factors for absorbed dose in a mobile phone to absorbed dose in critical organs in an anthropomorphic phantom for emergency dosimetry applications: OSL and TL experimental results, and Monte Carlo simulations. **Radiat Meas,** in press, doi: https://doi.org/10.1016/j.radmeas.2022.106781, 2022.

[7] SMITH, R.W., EAKINS, J.S., HAGER, L.G., ROTHKAMM, K., TANNER, R.J. Development of a retrospective/fortuitous accident dosimetry service based on OSL of mobile phones. **Radiat Protect Dosim,** v. 164, p. 89–92, 2015.

[8] SHOLOM, S., MCKEEVER, S.W.S. Developments for emergency dosimetry using components of mobile phones. **Radiat Meas,** v. 106, p. 416–422, 2017.

[9] SHOLOM, S., MCKEEVER, S.W.S. OSL with chips from US credit cards. **Radiat Meas,** v. 141, p. 106536, 2021.

[10] BASSINET, C., WODA, C., BORTOLIN, E., DELLA MONACA, S., FATTIBENE, P., QUATTRINI, M.S., BULANEK, B., EKENDAHL, D., BURBIDGE, C., CAUWELS, V., KOUROUKLA, E., GEBER-BERGSTRAND, T., MROZIK, A., MARCZEWSKA, B., BILSKI, P., SHOLOM, S., MCKEEVER, S.W.S., SMITH, R.W., VERONESE, I., GALLI, A., PANZERI, L., MARTINI, M. Retrospective radiation dosimetry using OSL from electronic components: results of an inter-laboratory comparison. **Radiat Meas,** v. 71, p. 475–479, 2014.

[11] MCKEEVER, S.W.S., SHOLOM, S. Luminescence measurements for retrospective dosimetry. In: CHEN, R., PAGONIS, V. (Eds.) **Advances in physics and applications of optically and thermally stimulated luminescence.** World Scientific Publishing Europe Ltd., 2019, p. 319–362.

[12] MCKEEVER, S.W.S., SHOLOM, S., CHANDLER, J.R. Developments in the use of thermoluminescence and optically stimulated luminescence from mobile phones in emergency dosimetry. **Radiat Protect Dosim,** v. 192, p. 205–235, 2020.

[13] CHANDLER, J.R., SHOLOM, S., MCKEEVER, S.W.S., HALL, H.L. Thermoluminescence and phototransferred thermoluminescence dosimetry on mobile phone protective touchscreen glass. **J Appl Phys,** v. 126, p. 074901, 2019.

[14] CHANDLER, J.R., SHOLOM, S., MCKEEVER, S.W.S., SEAGRAVES, D.T., HALL, H.L. Optically stimulated luminescence dosimetry on mobile phone back protective glass. **Phys Open,** v. 7, p. 100072, 2021.

[15] SHOLOM, S., MCKEEVER, S.W.S., CHANDLER, J.R. OSL dosimetry with protective glasses of modern smartphones: a fiber-optic, non-destructive approach. **Radiat Meas,** v. 136, p. 106382, 2020.

[16] SHOLOM, S., MCKEEVER, S.W.S. A non-destructive, high-sensitivity, emergency dosimetry method using OSL from protective back-glasses from smartphones. **Radiat Meas,** v. 147, p. 106646, 2022.

[17] HUNTLEY, D.J. An explanation of the power-law decay of luminescence. **J Phys Condens Matter,** v. 18, p. 1359–1365, 2006.

[18] JAIN, M., GURALNIK, B., ANDERSEN, M.T. Stimulated luminescence emission from localized recombination in randomly distributed defects. **J Phys Condens Matter,** v. 24, p. 385402, 2012.

[19] KITIS, G., PAGONIS, V. Analytical solutions for stimulated luminescence emission from tunneling recombination in random distributions of defects. **J Lumin,** v. 137, p. 109–115, 2012.

[20] KARS, R.H., POOLTON, N.R.J., JAIN, M., ANJÆRGAARD, C., DORENBOS, P., WALLINDA, J. On the trap depth of the IR-sensitive trap in Na and K-feldpsar. **Radiat Meas,** v. 59, p. 103–113, 2013.